Eur. Phys. J. C (2009) 64: 243–250
DOI 10.1140/epjc/s10052-009-1157-1

THE EUROPEAN PHYSICAL JOURNAL C

Regular Article - Experimental Physics

Experimental studies of $e^+e^- \to$ some charmless processes containing K^0_S at $\sqrt{s} = 3.773$ and 3.65 GeV

The BES Collaboration

M. Ablikim[1], L. An[2], J.Z. Bai[1], Y. Bai[1], Y. Ban[3], X. Cai[1], H.F. Chen[4], H.S. Chen[1], H.X. Chen[1], J.C. Chen[1], J. Chen[1], X.D. Chen[5], Y.B. Chen[1], Y.P. Chu[1], Y.S. Dai[6], Z.Y. Deng[1], S.X. Du[1,7], J. Fang[1], C.D. Fu[1], C.S. Gao[1], Y.N. Gao[8], S.D. Gu[1], Y.T. Gu[2], Y.N. Guo[1], K.L. He[1], M. He[9], Y.K. Heng[1], H.M. Hu[1], T. Hu[1], G.S. Huang[1,10], X.T. Huang[9], Y.P. Huang[1], X.B. Ji[1], L.L. Jiang[1], X.S. Jiang[1], J.B. Jiao[9], D.P. Jin[1], S. Jin[1], G. Li[1], H.B. Li[1], J. Li[1], L. Li[1], R.Y. Li[1], W.D. Li[1], W.G. Li[1], X.L. Li[1], X.N. Li[1], X.Q. Li[11], Y.F. Liang[12], B.J. Liu[1,13], C.X. Liu[1], F. Liu[1], F. Liu[14], H.M. Liu[1], J.P. Liu[15], H.B. Liu[2,16], J. Liu[1], R.G. Liu[1], S. Liu[17], Z.A. Liu[1], F. Lu[1], G.R. Lu[5], J.G. Lu[1], C.L. Luo[18], F.C. Ma[17], H.L. Ma[1], Q.M. Ma[1], M.Q.A. Malik[1], Z.P. Mao[1], X.H. Mo[1], J. Nie[1], R.G. Ping[1], N.D. Qi[1], J.F. Qiu[1], G. Rong[1], X.D. Ruan[2], L.Y. Shan[1], L. Shang[1], X.Y. Shen[1], H.Y. Sheng[1], H.S. Sun[1], S.S. Sun[1], Y.Z. Sun[1], Z.J. Sun[1], X. Tang[1], J.P. Tian[8], G.L. Tong[1], X. Wan[1], L. Wang[1], L.L. Wang[1], L.S. Wang[1], P. Wang[1], P.L. Wang[1], Y.F. Wang[1], Z. Wang[1], Z.Y. Wang[1], C.L. Wei[1], D.H. Wei[19], N. Wu[1], X.M. Xia[1], G.F. Xu[1], X.P. Xu[14], Y. Xu[11], M.L. Yan[4], H.X. Yang[1], M. Yang[1], Y.X. Yang[19], M.H. Ye[20], Y.X. Ye[4], C.X. Yu[11], C.Z. Yuan[1], Y. Yuan[1], Y. Zeng[21], B.X. Zhang[1], B.Y. Zhang[1], C.C. Zhang[1], D.H. Zhang[1], H.Q. Zhang[1], H.Y. Zhang[1], J.W. Zhang[1], J.Y. Zhang[1], X.Y. Zhang[9], Y.Y. Zhang[12], Z.X. Zhang[3], Z.P. Zhang[4], D.X. Zhao[1], J.W. Zhao[1], M.G. Zhao[1], P.P. Zhao[1], B. Zheng[1], H.Q. Zheng[3], J.P. Zheng[1], Z.P. Zheng[1], B. Zhong[18], L. Zhou[1], K.J. Zhu[1], Q.M. Zhu[1], X.W. Zhu[1], Y.S. Zhu[1], Z.A. Zhu[1], Z.L. Zhu[19], B.A. Zhuang[1], B.S. Zou[1]

[1] Institute of High Energy Physics, Beijing 100049, People's Republic of China
[2] Guangxi University, Nanning 530004, People's Republic of China
[3] Peking University, Beijing 100871, People's Republic of China
[4] University of Science and Technology of China, Hefei 230026, People's Republic of China
[5] Henan Normal University, Xinxiang 453002, People's Republic of China
[6] Zhejiang University, Hangzhou 310028, People's Republic of China
[7] *Present address:* Zhengzhou University, Zhengzhou 450001, People's Republic of China
[8] Tsinghua University, Beijing 100084, People's Republic of China
[9] Shandong University, Jinan 250100, People's Republic of China
[10] *Present address:* University of Oklahoma, Norman, OK 73019, USA
[11] Nankai University, Tianjin 300071, People's Republic of China
[12] Sichuan University, Chengdu 610064, People's Republic of China
[13] *Present address:* University of Hong Kong, Pok Fu Lam Road, Pok Fu Lam, Hong Kong
[14] Huazhong Normal University, Wuhan 430079, People's Republic of China
[15] Wuhan University, Wuhan 430072, People's Republic of China
[16] *Present address:* Graduate University of Chinese Academy of Sciences, Beijing 100049, People's Republic of China
[17] Liaoning University, Shenyang 110036, People's Republic of China
[18] Nanjing Normal University, Nanjing 210097, People's Republic of China
[19] Guangxi Normal University, Guilin 541004, People's Republic of China
[20] China Center for Advanced Science and Technology (CCAST), Beijing 100080, People's Republic of China
[21] Hunan University, Changsha 410082, People's Republic of China

Received: 9 June 2009 / Revised: 19 August 2009 / Published online: 30 September 2009

Abstract We measure the observed cross sections for the charmless processes $e^+e^- \to K^0_S K^- K^- K^+ \pi^+ + c.c.$, $K^0_S K^- \pi^+ \eta + c.c.$, $K^0_S K^- \pi^+ \pi^+ \pi^- \eta + c.c.$, $K^0_S K^- K^- K^+ \pi^+ \eta + c.c.$, $K^0_S K^- K^- K^+ \pi^+ \pi^0 + c.c.$, $K^0_S K^- \rho^+ + c.c.$ and $K^0_S K^- \pi^+ \rho^0 + c.c.$ We also extract upper limits on the branching fractions for $\psi(3770)$ decays into these final states at 90% C.L. Analyzed data samples correspond to 17.3 pb^{-1} and 6.5 pb^{-1} integrated luminosities registered, respectively, at $\sqrt{s} = 3.773$ and 3.65 GeV, with the BES-II detector at the BEPC collider.

1 Introduction

Recently, experimental studies of $\psi(3770)$ decays and production become more and more attractive. Especially after the BES Collaboration observed the hadronic transition of $\psi(3770) \to J/\psi\pi^+\pi^-$ [1, 2], the BES and CLEO-c Collaborations made great progress in this field to quest for the exclusive non-$D\bar{D}$ decays of the $\psi(3770)$ [3–20]. Particularly, the BES Collaboration measured the branching fraction for $\psi(3770) \to$ non-$D\bar{D}$ to be $(14.7 \pm 3.2)\%$ [3–6, 21], which is beyond the predictions of those conventional theories which expect that more than 98% of $\psi(3770)$ decays into $D\bar{D}$. However, so far, the sum of the measured branching fractions for $\psi(3770) \to$ exclusive non-$D\bar{D}$ decays is still not more than 2% [1, 2, 14–17]. Two possibilities may lead to the abnormally large non-$D\bar{D}$ branching fraction. Either there may be some new structures or physics effects around the $\psi(3770)$ [22, 23], or there exist more non-$D\bar{D}$ decays of the $\psi(3770)$. Anyway, experimental studies of the charmless processes produced in e^+e^- annihilation around the $\psi(3770)$ may provide some helpful information.

In this paper, by analyzing the data samples collected at $\sqrt{s} = 3.773$ and 3.65 GeV with the BES-II detector at the BEPC collider, we study the charmless processes $K_S^0K^-K^-K^+\pi^+$ (throughout the paper, charge conjugation is implied), $K_S^0K^-\pi^+\eta$, $K_S^0K^-\pi^+\pi^+\pi^-\eta$, $K_S^0K^-K^-K^+\pi^+\eta$, $K_S^0K^-K^-K^+\pi^+\pi^0$, $K_S^0K^-\rho^+$ and $K_S^0K^-\pi^+\rho^0$ produced in e^+e^- annihilation.

2 The BES-II detector

The BES-II is a conventional cylindrical magnetic detector that is described in detail in [24, 25]. A 12-layer vertex chamber (VC) surrounding a beryllium beam pipe provides input to event trigger, as well as coordinate information. A forty-layer main drift chamber (MDC) located just outside the VC yields precise measurements of charged particle trajectories with a solid angle coverage of 85% of 4π; it also provides ionization energy loss (dE/dx) measurements for particle identification. Momentum resolution of $1.7\%\sqrt{1+p^2}$ (p in GeV/c) and dE/dx resolution of 8.5% for Bhabha scattering electrons are obtained for the data taken at $\sqrt{s} = 3.773$ GeV. An array of 48 scintillation counters surrounding the MDC measures the time of flight (TOF) of charged particles with a resolution of about 180 ps for electrons. Outside the TOF counters, a 12 radiation length, lead-gas barrel shower counter (BSC), operating in limited streamer mode, measures the energies of electrons and photons over 80% of the total solid angle with an energy resolution of $\sigma_E/E = 0.22/\sqrt{E}$ (E in GeV) and spatial resolutions of $\sigma_\phi = 7.9$ mrad and $\sigma_z = 2.3$ cm for electrons. A solenoidal magnet outside the BSC provides a 0.4 T magnetic field in the central tracking region of the detector. Three double-layer muon counters instrument the magnet flux return and serve to identify muons with momentum greater than 500 MeV/c. They cover 68% of the total solid angle.

3 Data and Monte Carlo

The integrated luminosities of the data samples taken at $\sqrt{s} = 3.773$ and 3.65 GeV are 17.3 pb^{-1} and 6.5 pb^{-1}, respectively, which were measured by analyzing the large angle Bhabha scattering events from the two data samples [3]. In this paper, we call the two data samples as the $\psi(3770)$ data and the continuum data, respectively.

In order to determine the detection efficiency of $e^+e^- \to$ *exclusive light hadrons* and estimate their backgrounds, we use Monte Carlo simulation. The Monte Carlo events of $e^+e^- \to$ *exclusive light hadrons* are generated by a phase space generator based on the Monte Carlo simulation for the BES-II detector [26]. The generator includes initial state radiation (ISR) and photon vacuum polarization corrections [27] with $1/s$ cross section energy dependence. The reduction of the detection efficiency, due to the effect of the final state radiation [28], is not more than 0.5%. The generator was used in previous analyses [9–13].

4 Analysis

To investigate the processes $e^+e^- \to K_S^0K^-K^-K^+\pi^+$, $K_S^0K^-\pi^+\eta$, $K_S^0K^-\pi^+\pi^+\pi^-\eta$, $K_S^0K^-K^-K^+\pi^+\eta$, $K_S^0K^-K^-K^+\pi^+\pi^0$, $K_S^0K^-\rho^+$ and $K_S^0K^-\pi^+\rho^0$, we reconstruct the K_S^0, η, π^0 and ρ particles through the decays $K_S^0 \to \pi^+\pi^-$, $\eta \to \gamma\gamma$, $\pi^0 \to \gamma\gamma$ and $\rho \to \pi\pi$, respectively.

4.1 Event selection criteria

To ensure well measured 3-momentum vectors and reliability of the charged particle identification, we require that all charged tracks used in the analysis satisfy the following selection criteria. All of them are reconstructed in the MDC with good helix fits. Each of them has a polar angle θ with respect to the beam axis satisfying $|\cos\theta| < 0.85$, and originates from the interaction region with $\sqrt{V_x^2 + V_y^2} < 2.0$ cm ($\sqrt{V_x^2 + V_y^2} < 8.0$ cm for those from K_S^0) and $|V_z| < 20.0$ cm. Here, V_x, V_y and V_z are the x, y and z coordinates of the point of the closest approach of the charged track relative to the beam axis. For particle identification, we use the combined dE/dx and TOF measurements of each charged track. With these measurements, we calculate the combined confidence level CL_π (or CL_K) under the assumption that the

charged track is a pion (or a kaon). We identify the charged track as a pion (or a kaon) if it satisfies $CL_\pi > 0.001$ (or $CL_K > CL_\pi$). To reconstruct K_S^0 mesons, we require that the $\pi^+\pi^-$ meson pair originate from a secondary vertex which is displaced from the event vertex at least by 4 mm in the xy-plane.

We select photons by using the BSC measurements. To suppress the background, if a neutral cluster satisfies the following selection criteria, we consider it as a good photon. The energy of the cluster deposited in the BSC is greater than 50 MeV, the electromagnetic shower starts in the first five readout layers, the angle between the cluster and the nearest charged track is greater than 22° [29–32] and the opening angle between the cluster development direction and the photon emission direction is less than 37° [29–32].

We perform an energy-momentum conservation kinematic fit on each combination, to improve track momentum resolution and suppress the background. For the final state $e^+e^- \to K_S^0 K^- \rho^+$, an additional mass constraint kinematic fit is imposed on the decay $\pi^0 \to \gamma\gamma$. Combinations with a χ^2 probability of the kinematic fit greater than 1% are kept. In each event, there may be more than one combination satisfying the above criteria for each process. Only the combination with the largest kinematic fit probability is retained.

Above the $D\bar{D}$ pair production threshold, $D\bar{D}$ decays may contaminate the processes in question. Here, we take the process $K_S^0 K^- \pi^+ \eta$ as an example. From this process, the D and $\bar{D}$ mesons can be reconstructed in the decay modes $D^- \to K_S^0 K^-$ and $D^+ \to \pi^+\eta$, $D^- \to K^-\eta$ and $D^+ \to K_S^0\pi^+$, $\bar{D}^0 \to K^-\pi^+$ and $\bar{D}^0 \to K_S^0\eta$. To exclude these background events, we use the double tag method [29]. Those events are rejected if they can be reconstructed in the above modes. For the other processes, the events from $D\bar{D}$ decays are suppressed by using the same method. The Monte Carlo study shows that the contributions from $D\bar{D}$ decays are almost eliminated entirely by this procedure. The remaining $D\bar{D}$ contributions are subtracted in Sect. 4.3.

4.2 Candidate events selected from the data sets

For K_S^0 reconstruction, we calculate the invariant masses ($M_{\pi^+\pi^-}$) of the $\pi^+\pi^-$ combinations. The mass window of $|M_{\pi^+\pi^-} - M_{K_S^0}| < 3\sigma_{M_{K_S^0}}$ is taken as the K_S^0 signal region, and the mass window of $4\sigma_{M_{K_S^0}} < |M_{\pi^+\pi^-} - M_{K_S^0}| < 7\sigma_{M_{K_S^0}}$ is taken as the K_S^0 sideband region, where $M_{K_S^0}$ is the K_S^0 nominal mass [21], $\sigma_{M_{K_S^0}}$ is the K_S^0 mass resolution determined by the Monte Carlo simulation. The events with $M_{\pi^+\pi^-}$ in the K_S^0 sideband region are used to estimate the combinatorial $\pi^+\pi^-$ background in the K_S^0 signal region.

4.2.1 *Candidates for* $e^+e^- \to K_S^0 K^- K^- K^+ \pi^+$

Figure 1 shows the distributions of the $\pi^+\pi^-$ invariant masses of the candidate events for $e^+e^- \to K_S^0 K^- K^- K^+ \pi^+$. In the figure, K_S^0 signals can be seen. Fitting the $\pi^+\pi^-$ invariant mass spectrum of Fig. 1(a) with a Gaussian function for the K_S^0 signal and a flat background, we obtain 6.1 ± 2.6 events for $e^+e^- \to K_S^0 K^- K^- K^+ \pi^+$ observed from the $\psi(3770)$ data. In Fig. 1(b), there is no event observed outside the K_S^0 signal region, we obtain 3.0 ± 1.7 events for $e^+e^- \to K_S^0 K^- K^- K^+ \pi^+$ from the continuum data, by counting the events with $M_{\pi^+\pi^-}$ in the K_S^0 signal region.

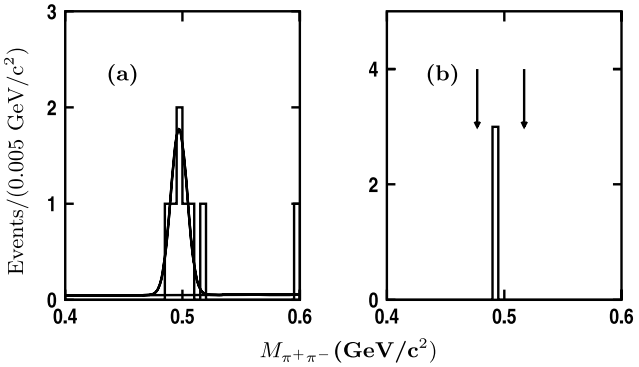

Fig. 1 Distributions of the $\pi^+\pi^-$ invariant masses of the candidate events for $e^+e^- \to K_S^0 K^- K^- K^+ \pi^+$ selected from (**a**) the $\psi(3770)$ data and (**b**) the continuum data, where the pair of arrows denotes the K_S^0 signal region

4.2.2 *Candidates for the processes containing* η *or* π^0

To select the candidate events for $e^+e^- \to K_S^0 K^-\pi^+\eta$, $K_S^0 K^-\pi^+\pi^+\pi^-\eta$, $K_S^0 K^- K^- K^+\pi^+\eta$ and $K_S^0 K^- K^- K^+\pi^+\pi^0$, we check the $\gamma\gamma$ invariant mass ($M_{\gamma\gamma}$) spectra for the events with $M_{\pi^+\pi^-}$ in the K_S^0 signal region. They are shown in Figs. 2 and 3. Fitting the spectrum in Fig. 2(a) with a Gaussian function for the η signal and a flat background yields 10.7 ± 4.0 η candidates. In the fit, the η mass is fixed to the PDG value [21] and the η resolution is fixed to the value determined by the Monte Carlo simulation. Via a similar analysis of the events in the K_S^0 sideband region, we obtain 1.5 ± 1.6 η candidates. After background subtraction, we obtain 9.2 ± 4.3 events for $e^+e^- \to K_S^0 K^-\pi^+\eta$ observed from the $\psi(3770)$ data.

In the other distributions, there is no obvious signal for η or π^0 observed. The mass window of $|M_{\gamma\gamma} - M_{\eta/\pi^0}| < 3\sigma_{M_{\eta/\pi^0}}$ is taken as the η/π^0 signal region, where M_{η/π^0} is the η/π^0 nominal mass [21], $\sigma_{M_{\eta/\pi^0}}$ is the η/π^0 mass resolution determined by the Monte Carlo simulation. By counting the events with $M_{\gamma\gamma}$ in the η or π^0 signal region, we obtain the number of events observed. For the processes $e^+e^- \to K_S^0 K^-\pi^+\pi^+\pi^-\eta$, $K_S^0 K^- K^- K^+\pi^+\eta$ and $K_S^0 K^- K^- K^+\pi^+\pi^0$, 7, 0 and 3 events are observed from the $\psi(3770)$ data. For the processes $e^+e^- \to K_S^0 K^-\pi^+\eta$, $K_S^0 K^-\pi^+\pi^+\pi^-\eta$, $K_S^0 K^- K^- K^+\pi^+\eta$ and

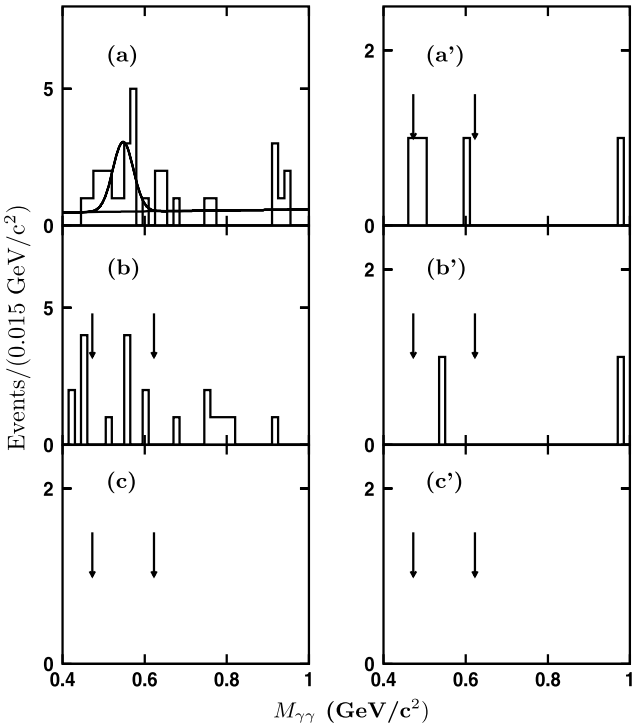

Fig. 2 Distributions of the $\gamma\gamma$ invariant masses of the candidate events for $e^+e^- \to$ (**a**) $K^0_S K^-\pi^+\eta$, (**b**) $K^0_S K^-\pi^+\pi^+\pi^-\eta$ and (**c**) $K^0_S K^-K^-K^+\pi^+\eta$, by requiring that $M_{\pi^+\pi^-}$ be in the K^0_S signal region, selected from the $\psi(3770)$ data (*left*) and the continuum data (*right*), where the pair of arrows denotes the η signal region

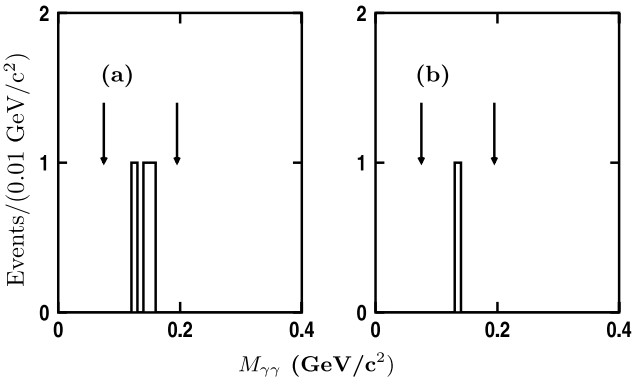

Fig. 3 Distributions of the $\gamma\gamma$ invariant masses of the candidate events for $e^+e^- \to K^0_S K^-K^+K^-\pi^+\pi^0$, by requiring that $M_{\pi^+\pi^-}$ be in the K^0_S signal region, selected from (**a**) the $\psi(3770)$ data and (**b**) the continuum data, where the pair of arrows denotes the π^0 signal region

$K^0_S K^-K^-K^+\pi^+\pi^0$, 3, 1, 0 and 1 event are observed from the continuum data. While, no event is observed in the K^0_S sideband region.

4.2.3 Candidates for the processes containing ρ^+ or ρ^0

Figure 4 shows the distributions of the $\pi^+\gamma\gamma$ or $\pi^+\pi^-$ invariant masses of the candidate events for $e^+e^- \to$ $K^0_S K^-\rho^+$ and $K^0_S K^-\pi^+\rho^0$ with $M_{\pi^+\pi^-}$ in the K^0_S signal region. Fitting the spectra in Figs. 4(a) and (b) with a Gaussian function convoluted with a Breit-Wigner function for the ρ signal and using a 0-order or 2-order polynomial background, respectively, yields the fitted number $N^{\rho,\mathrm{fit}}_{K^0_S\mathrm{sig}}$ of ρ candidates. In the fit, the ρ mass and width are fixed to the PDG values [21], and the ρ mass resolution is fixed to the value determined by the Monte Carlo simulation.

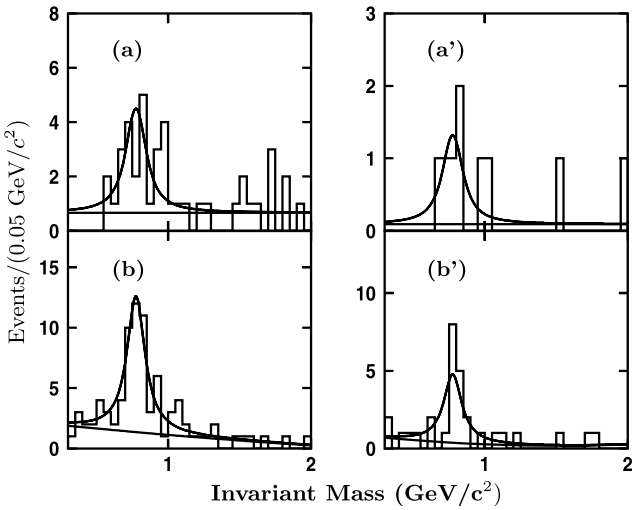

Fig. 4 Distributions of the $\pi^+\gamma\gamma$ or $\pi^+\pi^-$ invariant masses of the candidate events for $e^+e^- \to$ (**a**) $K^0_S K^-\rho^+$ and (**b**) $K^0_S K^-\pi^+\rho^0$, by requiring that $M_{\pi^+\pi^-}$ be in the K^0_S signal region, selected from the $\psi(3770)$ data (*left*) and the continuum data (*right*)

There may be combinatorial $\pi^+\pi^-$ background in the K^0_S signal region. To estimate such background, we investigate the events with $M_{\pi^+\pi^-}$ in the K^0_S sideband region. A similar analysis gives the fitted number $N^{\rho,\mathrm{fit}}_{K^0_S\mathrm{sid}}$ of ρ candidates from the K^0_S sideband region.

For $e^+e^- \to K^0_S K^-\rho^+$, we can determine the number N^{obs} of events by

$$N^{\mathrm{obs}} = N^{\rho^+,\mathrm{fit}}_{K^0_S\mathrm{sig}} - N^{\rho^+,\mathrm{fit}}_{K^0_S\mathrm{sid}}. \quad (1)$$

For $e^+e^- \to K^0_S K^-\pi^+\rho^0$, however, there are two $\pi^+\pi^-$ combinations which can enter the $\pi^+\pi^-$ invariant mass spectrum in Fig. 4(b), since it is reconstructed by the final state $K^0_S K^-\pi^+\pi^+\pi^-$. The numbers of such multiple entries need be subtracted from the fitted numbers $N^{\rho^0,\mathrm{fit}}_{K^0_S\mathrm{sig}}$ and $N^{\rho^0,\mathrm{fit}}_{K^0_S\mathrm{sid}}$ of ρ^0 candidates, respectively. They are obtained by counting the events in Fig. 4(b).

In the ρ^0 signal region, however, the multiple entries are from the ρ^0 signal and the combinatorial background. To estimate the number of multiple entries in the combinatorial background, we need know the rate of multiple entries in the combinatorial background. This rate can be expected by

Table 1 The numbers $N^{\rm obs}$ of events for $e^+e^- \to K^0_S K^- \rho^+$ and $K^0_S K^- \pi^+ \rho^0$ observed from the $\psi(3770)$ data and the continuum data, where, $N^{\rho,\rm fit}_{K^0_S \rm sig}$ and $N^{\rho,\rm fit}_{K^0_S \rm sid}$ are the fitted numbers of ρ candidates; $N^{\rm mult}_{K^0_S \rm sig}$ and $N^{\rm mult}_{K^0_S \rm sid}$ are the numbers of multiple combinations in the ρ^0 signal region; which are obtained by analyzing the events in the K^0_S signal region and sideband region, respectively

$e^+e^- \to$	Data	$N^{\rho,\rm fit}_{K^0_S \rm sig}$	$N^{\rm mult}_{K^0_S \rm sig}$	$N^{\rho,\rm fit}_{K^0_S \rm sid}$	$N^{\rm mult}_{K^0_S \rm sid}$	$N^{\rm obs}$
$K^0_S K^- \rho^+$	$\psi(3770)$	18.5 ± 5.9	–	0	–	18.5 ± 5.9
	Continuum	5.9 ± 2.9	–	0	–	5.9 ± 2.9
$K^0_S K^- \pi^+ \rho^0$	$\psi(3770)$	49.7 ± 9.9	21	6.0 ± 4.3	3	25.7 ± 11.8
	Continuum	19.4 ± 5.8	7	0	0	12.4 ± 6.4

the events in the ρ^0 sideband region. Here, the mass window between 0.4755 and 1.0755 GeV/c^2 is taken as the ρ^0 signal region, and the mass range from 1.1505 to 1.7505 GeV/c^2 is taken as the ρ^0 sideband region. Whereas, the detailed analysis shows that there is no multiple entry in the ρ^0 sideband region. So, we suppose that there is no multiple entry in the combinatorial background. This means that the multiple entries in the ρ^0 signal region are from the ρ^0 signal completely. Therefore, we can obtain the net number of ρ^0 candidates observed from the events in the K^0_S signal/sideband region by

$$N^{\rho^0,\rm net}_{K^0_S \rm sig/sid} = N^{\rho^0,\rm fit}_{K^0_S \rm sig/sid} - N^{\rm mult}_{K^0_S \rm sig/sid},$$

where, $N^{\rho^0,\rm fit}_{K^0_S \rm sig/sid}$ is the fitted number of ρ^0 candidates, and $N^{\rm mult}_{K^0_S \rm sig/sid}$ is the number of multiple entries. Then, we can determine the number $N^{\rm obs}$ of events for $e^+e^- \to K^0_S K^- \pi^+ \rho^0$ by

$$N^{\rm obs} = N^{\rho^0,\rm net}_{K^0_S \rm sig} - N^{\rho^0,\rm net}_{K^0_S \rm sid}. \quad (2)$$

Table 1 summarizes the numbers $N^{\rm obs}$ of events for $e^+e^- \to K^0_S K^- \rho^+$ and $K^0_S K^- \pi^+ \rho^0$ observed from the data.

4.3 Estimate of other backgrounds

In previous subsections, we have taken into account the combinatorial $\pi^+\pi^-$ background in the K^0_S signal region; and have rejected the dominant contributions from $D\bar{D}$ decays by using the double tag methods. While, there are still some other kinds of backgrounds in the selected candidate events for $e^+e^- \to$ *exclusive light hadrons*. Some events from J/ψ and $\psi(3686)$ decays produced due to ISR returns, from other processes due to particle misidentification between charged kaon and pion or due to missing photon(s) and from the remaining contributions of $D\bar{D}$ decays can satisfy the selection criteria for each process in question. We estimate the number $N^{\rm b}$ of such background events by using the same method as the one used in our previous works [9–13]. The details about the estimate of these backgrounds, which are based on the Monte Carlo simulation, were presented in [9].

5 Results

5.1 Observed cross sections

At the center-of-mass energies of 3.773 and 3.65 GeV, the experimentally observed events for $e^+e^- \to$ *exclusive light hadrons* not only include those from continuum production but also those from resonance production. In this analysis, we neglect the possible interference between the continuum amplitude and the resonance amplitude, as well as the difference of the vacuum polarization corrections at the two energy points. Under this condition, subtracting the number $N^{\rm b}$ of background events from the number $N^{\rm obs}$ of events observed, we obtain the number $N^{\rm net}$ of signal events for $e^+e^- \to f$.

Using the yield $N^{\rm net}$ and the reconstruction efficiency ϵ of the exclusive light hadron final state $e^+e^- \to f$, as well as the integrated luminosity $\mathcal{L}$ of the data sample, we can determine the observed cross section by

$$\sigma_{e^+e^- \to f} = \frac{N^{\rm net}}{\mathcal{L} \times \epsilon \times \mathcal{B}}, \quad (3)$$

where, $\mathcal{B}$ is the item accounting for the decay branching fractions for the daughter particles of K^0_S, η, π^0 and ρ since they have not been included in the determination of the detection efficiency. Table 2 summarizes the definitions of $\mathcal{B}$ for different channels.

The observed cross sections for some processes are determined. For the other processes, no or only a few events are observed in the data, we set upper limits $N^{\rm up}$ on the numbers of events for these processes at 90% confidence level (C.L.) by the Feldman-Cousins method [33]. Here, we assume that the background is absent. Then, we set upper limits on the

observed cross sections for these processes after considering systematic uncertainties.

In the cross section measurements, the systematic uncertainty is arising from the uncertainties in the integrated luminosity (∼2.1% [3]), the photon selection (∼2.0% per photon), the tracking efficiency (∼2.0% per track), the particle identification (∼0.5% per pion or kaon), the kinematic fit (∼1.5% [29]), the K_S^0 reconstruction (∼1.1% [32]), the Monte Carlo statistics (∼[1.9–3.0]%), the branching fraction quoted from PDG [21] (∼0.51% for $\mathcal{B}(\eta \to \gamma\gamma)$, ∼0.03% for $\mathcal{B}(\pi^0 \to \gamma\gamma)$, ∼0.07% for $\mathcal{B}(K_S^0 \to \pi^+\pi^-)$), the background estimation (∼[0–1.7]%), the fit to the mass spectrum (∼[0–2.8]%), and the Monte Carlo modeling (∼6.0% [9]). Adding these uncertainties in quadrature yields the total systematic uncertainty $\Delta_{\rm sys}$ for each process. For the cross section measurements at $\sqrt{s}$ = 3.773 and 3.65 GeV, the independent systematic uncertainty is from the uncertainties in the Monte Carlo statistics, the fit to the mass spectrum and the background estimation, while the common systematic uncertainty is from the other uncertainties.

The numbers of $N^{\rm obs}$, $N^{\rm b}$, $N^{\rm net}$ (or $N^{\rm up}$), ϵ, $\Delta_{\rm sys}$ and σ (or $\sigma^{\rm up}$) are summarized in Tables 3 and 4.

Table 2 Definitions of $\mathcal{B}$ for different channels, where, $\mathcal{B}_{K_S^0\to\pi^+\pi^-}$, $\mathcal{B}_{\eta\to\gamma\gamma}$, $\mathcal{B}_{\pi^0\to\gamma\gamma}$, $\mathcal{B}_{\rho^0\to\pi^+\pi^-}$ and $\mathcal{B}_{\rho^+\to\pi^+\pi^0}$ are the branching fractions for the decays $K_S^0 \to \pi^+\pi^-$, $\eta \to \gamma\gamma$, $\pi^0 \to \gamma\gamma$, $\rho^0 \to \pi^+\pi^-$ and $\rho^+ \to \pi^+\pi^0$, respectively

$e^+e^- \to$	$\mathcal{B}$
$K_S^0K^-K^-K^+\pi^+$	$\mathcal{B}_{K_S^0\to\pi^+\pi^-}$
$K_S^0K^-\pi^+\eta$	$\mathcal{B}_{K_S^0\to\pi^+\pi^-} \times \mathcal{B}_{\eta\to\gamma\gamma}$
$K_S^0K^-\pi^+\pi^+\pi^-\eta$	$\mathcal{B}_{K_S^0\to\pi^+\pi^-} \times \mathcal{B}_{\eta\to\gamma\gamma}$
$K_S^0K^-K^-K^+\pi^+\eta$	$\mathcal{B}_{K_S^0\to\pi^+\pi^-} \times \mathcal{B}_{\eta\to\gamma\gamma}$
$K_S^0K^-K^-K^+\pi^+\pi^0$	$\mathcal{B}_{K_S^0\to\pi^+\pi^-} \times \mathcal{B}_{\pi^0\to\gamma\gamma}$
$K_S^0K^-\rho^+$	$\mathcal{B}_{K_S^0\to\pi^+\pi^-} \times \mathcal{B}_{\rho^+\to\pi^+\pi^0} \times \mathcal{B}_{\pi^0\to\gamma\gamma}$
$K_S^0K^-\pi^+\rho^0$	$\mathcal{B}_{K_S^0\to\pi^+\pi^-} \times \mathcal{B}_{\rho^0\to\pi^+\pi^-}$

5.2 Upper limits on the observed cross section and the branching fraction for $\psi(3770) \to f$

Usually, it is anticipated that there is only one simple $\psi(3770)$ and there are no other unknown structures and dynamics effects in the energy range from 3.70 to 3.89 GeV. If so, the contribution of the continuum production of each process at $\sqrt{s} = 3.773$ GeV can be expected from the measurement at $\sqrt{s} = 3.65$ GeV. The observed cross section $\sigma_{\psi(3770)\to f}$ for $\psi(3770) \to f$ can be determined by

$$\sigma_{\psi(3770)\to f} = \sigma_{e^+e^-\to f}^{3.773\ \rm GeV} - f_s \times \sigma_{e^+e^-\to f}^{3.65\ \rm GeV}, \quad (4)$$

Table 3 Observed cross sections for $e^+e^- \to$ *exclusive light hadrons* at $\sqrt{s} = 3.773$ GeV, where $N^{\rm obs}$ is the number of events observed, $N^{\rm b}$ is the number of all backgrounds, $N^{\rm net}$ is the number of signal events, $N^{\rm up}$ is the upper limit on the number of events set at 90% C.L., ϵ is the detection efficiency which does not include the branching fractions for the daughter particle decays, $\Delta_{\rm sys}$ is the relative systematic error, $\sigma^{\rm obs}$ is the observed cross section and $\sigma^{\rm up}$ is the cross section upper limit set at 90% C.L.

$e^+e^- \to$	$N^{\rm obs}$	$N^{\rm b}$	$N^{\rm net}$ (or $N^{\rm up}$)	ϵ [%]	$\Delta_{\rm sys}$ [%]	σ (or $\sigma^{\rm up}$) [pb]
$K_S^0K^-K^-K^+\pi^+$	6.1 ± 2.6	0.1 ± 0.1	6.0 ± 2.6	1.79 ± 0.04	14.5	$28.0 \pm 12.1 \pm 4.1$
$K_S^0K^-\pi^+\eta$	9.2 ± 4.3	0.0 ± 0.0	9.2 ± 4.3	3.72 ± 0.07	11.8	$52.6 \pm 24.6 \pm 6.2$
$K_S^0K^-\pi^+\pi^+\pi^-\eta$	7	–	<12.53	0.96 ± 0.02	14.7	<325.1
$K_S^0K^-K^-K^+\pi^+\eta$	0	–	<2.44	0.40 ± 0.01	14.8	<152.1
$K_S^0K^-K^-K^+\pi^+\pi^0$	3	–	<7.42	0.36 ± 0.01	14.9	<204.8
$K_S^0K^-\rho^+$	18.5 ± 5.9	0.3 ± 0.1	18.2 ± 5.9	3.35 ± 0.09	11.8	$45.9 \pm 14.9 \pm 5.4$
$K_S^0K^-\pi^+\rho^0$	25.7 ± 11.8	0.2 ± 0.2	25.5 ± 11.8	2.27 ± 0.06	14.4	$93.8 \pm 43.4 \pm 13.5$

Table 4 Observed cross sections for $e^+e^- \to$ *exclusive light hadrons* at $\sqrt{s} = 3.65$ GeV, where the definitions of the symbols are the same as those in Table 3

$e^+e^- \to$	$N^{\rm obs}$	$N^{\rm b}$	$N^{\rm net}$ (or $N^{\rm up}$)	ϵ [%]	$\Delta_{\rm sys}$ [%]	σ (or $\sigma^{\rm up}$) [pb]
$K_S^0K^-K^-K^+\pi^+$	3.0 ± 1.7	0.0 ± 0.0	3.0 ± 1.7	1.95 ± 0.05	14.2	$34.2 \pm 19.4 \pm 4.9$
$K_S^0K^-\pi^+\eta$	3	–	<7.42	3.87 ± 0.07	11.4	<122.4
$K_S^0K^-\pi^+\pi^+\pi^-\eta$	1	–	<4.36	1.02 ± 0.02	14.9	<284.1
$K_S^0K^-K^-K^+\pi^+\eta$	0	–	<2.44	0.41 ± 0.01	15.4	<397.8
$K_S^0K^-K^-K^+\pi^+\pi^0$	1	–	<4.36	0.36 ± 0.01	16.6	<326.8
$K_S^0K^-\rho^+$	5.9 ± 2.9	0.0 ± 0.0	5.9 ± 2.9	3.33 ± 0.08	11.6	$39.9 \pm 19.6 \pm 4.7$
$K_S^0K^-\pi^+\rho^0$	12.4 ± 6.4	0.0 ± 0.0	12.4 ± 6.4	2.36 ± 0.07	15.6	$116.8 \pm 60.3 \pm 18.2$

Table 5 Upper limits $\mathcal{B}^{\rm up}_{\psi(3770)\to f}$ on the branching fractions for $\psi(3770)\to f$ set at 90% C.L. In the table, $\sigma_{\psi(3770)\to f}$ is the measured observed cross section for $\psi(3770)\to f$, where the first error is statistical, the second is the independent systematic error and the third is the common systematic error; $\sigma^{\rm up}_{\psi(3770)\to f}$ is the upper limit on $\sigma_{\psi(3770)\to f}$. For the processes $K^0_S K^-\pi^+\pi^+\pi^-\eta$, $K^0_S K^- K^- K^+\pi^+\eta$ and $K^0_S K^- K^- K^+\pi^+\pi^0$, $\sigma^{\rm up}_{\psi(3770)\to f}$ is set by the observed cross section upper limit $\sigma^{\rm up}$ for $e^+e^-\to f$ at $\sqrt{s}$ = 3.773 GeV set at 90% C.L.; for the other processes, $\sigma^{\rm up}_{\psi(3770)\to f}$ is set at 90% C.L. under the hypothesis of a Gaussian distribution

Decay modes	$\sigma_{\psi(3770)\to f}$ [pb]	$\sigma^{\rm up}_{\psi(3770)\to f}$ [pb]	$\mathcal{B}^{\rm up}_{\psi(3770)\to f}$
$K^0_S K^- K^- K^+\pi^+$	$-4.0\pm21.8\pm1.3\pm0.6$	<33.5	$<4.9\times10^{-3}$
$K^0_S K^-\pi^+\eta$	$52.6\pm24.6\pm1.8\pm5.9$	<85.4	$<1.3\times10^{-2}$
$K^0_S K^-\pi^+\pi^+\pi^-\eta$	–	<325.1	$<4.8\times10^{-2}$
$K^0_S K^- K^- K^+\pi^+\eta$	–	<152.1	$<2.2\times10^{-2}$
$K^0_S K^- K^- K^+\pi^+\pi^0$	–	<204.8	$<3.0\times10^{-2}$
$K^0_S K^-\rho^+$	$8.6\pm23.6\pm1.8\pm1.0$	<44.6	$<6.6\times10^{-3}$
$K^0_S K^-\pi^+\rho^0$	$-15.5\pm71.2\pm4.8\pm2.2$	<108.3	$<1.6\times10^{-2}$

where, $\sigma^{3.773\ \rm GeV}_{e^+e^-\to f}$ and $\sigma^{3.65\ \rm GeV}_{e^+e^-\to f}$ are the measured observed cross sections for $e^+e^-\to f$ at $\sqrt{s}=3.773$ and 3.65 GeV, respectively; f_s is the normalization factor for the $1/s$ dependence of the cross section. The second column of Table 5 summarizes the results of $\sigma_{\psi(3770)\to f}$, where the first error is statistical, the second is the independent systematic error and the third is the common systematic error. For the final states $K^0_S K^-\pi^+\eta$, $K^0_S K^-\pi^+\pi^+\pi^-\eta$, $K^0_S K^- K^- K^+\pi^+\eta$ and $K^0_S K^- K^- K^+\pi^+\pi^0$, we neglect the contribution of the continuum production.

For the final states $K^0_S K^-\pi^+\pi^+\pi^-\eta$, $K^0_S K^- K^- K^+\pi^+\eta$ and $K^0_S K^- K^- K^+\pi^+\pi^0$, only a few events are observed from the $\psi(3770)$ data, we set upper limit $\sigma^{\rm up}_{\psi(3770)\to f}$ on the cross section for $\psi(3770)\to f$ at $\sqrt{s}$ = 3.773 GeV by $\sigma^{\rm up}$, which is upper limit on the cross section for $e^+e^-\to f$ at $\sqrt{s}$ = 3.773 GeV set at 90% C.L. For the other final states, we set $\sigma^{\rm up}_{\psi(3770)\to f}$ at 90% C.L. by assuming that $\sigma_{\psi(3770)\to f}$ follows a Gaussian distribution. They are summarized in the third column of Table 5.

The BES Collaboration has measured the observed cross section for $\psi(3770)$ production at $\sqrt{s}=3.773$ GeV to be $\bar{\sigma}^{\rm obs}_{\psi(3770)}=(7.15\pm0.27\pm0.27)$ nb [4, 9, 34]. Dividing $\sigma^{\rm up}_{\psi(3770)\to f}$ by $\bar{\sigma}^{\rm obs}_{\psi(3770)}$ and considering the systematic uncertainty, we set upper limit $\mathcal{B}^{\rm up}_{\psi(3770)\to f}$ on the branching fraction for $\psi(3770)\to f$ at 90% C.L., as summarized in the last column of Table 5.

6 Summary

In summary, by analyzing the data sets collected at $\sqrt{s}=$ 3.773 and 3.65 GeV with the BES-II detector at the BEPC collider, we have measured the observed cross sections for the charmless processes $K^0_S K^- K^- K^+\pi^+$, $K^0_S K^-\pi^+\eta$, $K^0_S K^-\pi^+\pi^+\pi^-\eta$, $K^0_S K^- K^- K^+\pi^+\eta$, $K^0_S K^- K^- K^+\pi^+\pi^0$, $K^0_S K^-\rho^+$ and $K^0_S K^-\pi^+\rho^0$ produced in e^+e^- annihilation at the two energy points. Using these measurements, we set upper limits on the branching fractions for $\psi(3770)$ decays into these final states at 90% C.L. These provide some helpful information to understand the mechanism of the continuum light hadron production and the $\psi(3770)$ non-$D\bar{D}$ decays.

Acknowledgements The BES collaboration thanks the staff of BEPC for their hard efforts. This work is supported in part by the National Natural Science Foundation of China under contracts Nos. 10491300, 10225524, 10225525, 10425523, 10935007, the Chinese Academy of Sciences under contract No. KJ 95T-03, the 100 Talents Program of CAS under Contract Nos. U-11, U-24, U-25, the Knowledge Innovation Project of CAS under Contract Nos. U-602, U-34 (IHEP), the National Natural Science Foundation of China under Contract No. 10225522 (Tsinghua University). This work is also supported by Young Innovation Fund of IHEP (No. H95461E).

References

1. J.Z. Bai et al. (BES Collaboration), High Energy Phys. Nucl. Phys. **28**(4), 325 (2004)
2. J.Z. Bai et al. (BES Collaboration), Phys. Lett. B **605**, 63 (2005)
3. M. Ablikim et al. (BES Collaboration), Phys. Lett. B **641**, 145 (2006)
4. M. Ablikim et al. (BES Collaboration), Phys. Rev. Lett. **97**, 121801 (2006)
5. M. Ablikim et al. (BES Collaboration), Phys. Lett. B **659**, 74 (2008)
6. M. Ablikim et al. (BES Collaboration), Phys. Rev. D **76**, 122002 (2007)
7. M. Ablikim et al. (BES Collaboration), Phys. Rev. D **70**, 077101 (2004)
8. M. Ablikim et al. (BES Collaboration), Phys. Rev. D **72**, 072007 (2005)
9. M. Ablikim et al. (BES Collaboration), Phys. Lett. B **650**, 111 (2007)
10. M. Ablikim et al. (BES Collaboration), Phys. Lett. B **656**, 30 (2007)
11. M. Ablikim et al. (BES Collaboration), Eur. Phys. J. C **52**, 805 (2007)
12. M. Ablikim et al. (BES Collaboration), Phys. Lett. B **670**, 179 (2008)

13. M. Ablikim et al. (BES Collaboration), Phys. Lett. B **670**, 184 (2008)
14. N.E. Adam et al. (CLEO Collaboration), Phys. Rev. Lett. **96**, 082004 (2006)
15. T.E. Coans et al. (CLEO Collaboration), Phys. Rev. Lett. **96**, 182002 (2006)
16. R.A. Briere et al. (CLEO Collaboration), Phys. Rev. D **74**, 031106 (2006)
17. G.S. Adams et al. (CLEO Collaboration), Phys. Rev. D **73**, 012002 (2006)
18. D. Cronin-Hennessy et al. (CLEO Collaboration), Phys. Rev. D **74**, 012005 (2006)
19. D. Besson et al. (CLEO Collaboration), Phys. Rev. Lett. **96**, 092002 (2006)
20. G.S. Huang et al. (CLEO Collaboration), Phys. Rev. Lett. **96**, 032003 (2006)
21. C. Amsler et al. (Particle Data Group), Phys. Lett. B **667**, 1 (2008)
22. M. Ablikim et al. (BES Collaboration), Phys. Rev. Lett. **101**, 102004 (2008)
23. M. Ablikim et al. (BES Collaboration), Phys. Lett. B **668**, 263 (2008)
24. J.Z. Bai et al. (BES Collaboration), Nucl. Instrum. Methods A **344**, 319 (1994)
25. J.Z. Bai et al. (BES Collaboration), Nucl. Instrum. Methods A **458**, 627 (2001)
26. M. Ablikim et al. (BES Collaboration), Nucl. Instrum. Methods A **552**, 344 (2005)
27. E.A. Kuraev, V.S. Fadin, Yad. Fiz. **41**, 733 (1985)
28. E. Barberio, Z. Wąs, Comput. Phys. Commun. **79**, 291 (1994)
29. M. Ablikim et al. (BES Collaboration), Nucl. Phys. B **727**, 395 (2005)
30. M. Ablikim et al. (BES Collaboration), Phys. Lett. B **597**, 39 (2004)
31. M. Ablikim et al. (BES Collaboration), Phys. Lett. B **603**, 130 (2004)
32. M. Ablikim et al. (BES Collaboration), Phys. Lett. B **608**, 24 (2005)
33. G.J. Feldman, R.D. Cousins, Phys. Rev. D **57**, 3873 (1998)
34. M. Ablikim et al. (BES Collaboration), Phys. Lett. B **652**, 238 (2007)